Light Scattering from Rough Thin Films: DDA Simulations

Hannu Parviainen and Kari Lumme

Observatory, P.O. box 14, FIN-00014, University of Helsinki, Finland
e-mail: hannu@astro.helsinki.fi

Abstract

Light scattering properties of rough thin circular films of constant thickness are studied using the discrete-dipole approximation. Effects on the intensity distribution of the scattered light due to different statistical roughness models, model dependant roughness parameter, and uncorrelated small-scale porosity of the inhomogeneous media are investigated. The effects due to inhomogeneity of the scattering media are compared with the analytic approximation by Maxwell Garnett and the results are found to agree well with the theory.

1 Introduction

The latest advances in computing power and numerical methods—such as the distribution of the geometry to different computing nodes as in the ADDA-code [1]—has allowed the DDA simulations of objects with ever extending sizes. We are approaching the range where we can study the wave-optic effects due to the rough boundaries between extended media of different physical properties (i.e. rough-surface scattering), together with the volume effects from the internal structure of the scattering media. This study considers computationally light rough-surface analogs, deformed thin circular films, which allow us to study the wave-optics effects due to surface roughness, and to investigate the volume scattering effects to some extent.

Rough Thin Films The film geometry is represented as a thin circular slab of constant thickness t along the z-axis. The deformation along the z-axis is modeled by a two-dimensional homogeneous isotropic random field $h(x, y)$ [2]. The distribution of heigths follows Gaussian statistics, and is defined by the standard deviation σ. The generation of the geometry realizations is based on the spectral synthesis method [3].

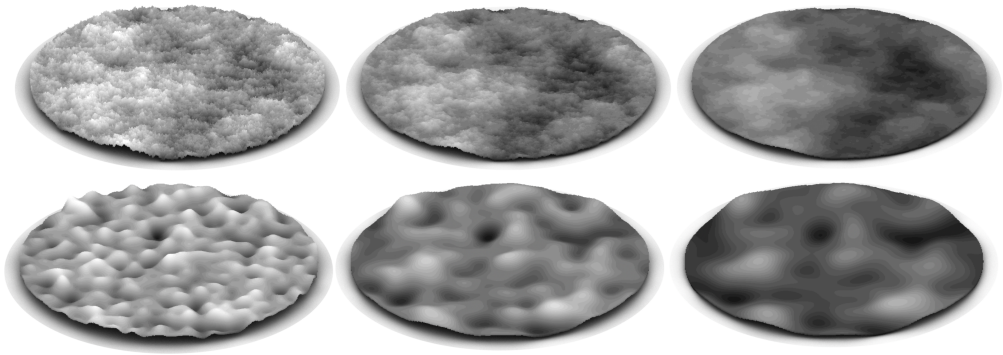

Figure 1: In the upper row we show the fBm model, in the lower the Gc model. Horizontal roughness parameter changes from left to right as $H = 0.25,\ 0.5,\ 0.9$ and $\frac{l}{L} = 0.215,\ 0.5,\ 0.75$.

As in [4], two different types of roughness models were chosen for the study: fractional Brownian motion (fBm) and Gaussian correlation (Gc). The two models are shown in Fig. 1. Gc-surfaces show roughness features of a certain scale, determined by the correlation length l, while the fBm-surfaces are of self-affine nature showing roughness features in all scales, distribution determined by the Hurst exponent H. For brevity, both l and H are denoted in the following text by a horizontal roughness parameter τ.

2 Simulations

2.1 Numerical Methods

Simulations were carried out using a modified version of the DDSCAT-code [5] by B. Draine, and the results were verified against the ADDA-code [1]. The modifications consisted of inclusion of several F90 features into the F70-code, such as dynamical allocation of memory for more convenient working with geometries of varying sizes. The modifications were tested not to affect the simulation results.

The geometry was discretized into cells of 0.025 μm width and height. The radius of the circular film was 5.0 μm, and the thickness of the film was set to 4 cells, corresponding to 0.1 μm. This discretization scheme leads to effective radius A_{eff} of 1.12, and size parameter x of 12.64 for the value of $\lambda = 0.557\mu m$ used in the simulations. Only the effects due to the horizontal roughness parameter were studied, and the amplitude of the roughness deformations in the z-axis was considered as constant, $\frac{\sigma}{L} = 0.01$.

Geometries with packing density $\rho < 1$ were generated by randomly removing $n \times n \times n$ dipole chunks from the solid geometries. While this method lacks the elegance of using, e.g., a random field to define ρ, it allows us to study the scattering dependency of the films due to the varying size of the voids in a simple and well-determinated manner.

The Sepeli computing cluster of the Finnish IT center for science (CSC) was used to carry out the simulations. The memory usage for a single geometry was around 4-6 GB, and computation time varied from several tens of minutes to hours, depening on the packing density and the index of refraction of the scattering medium.

2.2 Simulation Sets

The main focus of the study was on the the behaviour of the scattered intensity $M_{11}(\theta_i, \phi_i, \theta_e, \phi_e)$—where (θ_i, ϕ_i) are the angles of incidence, (θ_e, ϕ_e) the angles of emergence— as a function of the horizontal roughness parameter and composition of the scattering media. The simulations were divided into five sets, each studying different aspects of the scattering problem. For each value of the studied variable, the results are averaged over 30 geometry realizations to obtain statistically meaningful results. When possible (i.e., for normal incident radition, sets 1-4), the averaging is also carried out over 20 values of ϕ_e, thus giving $M_{11}(\theta_e)$ as an average of 600 samples.

Set 1 studied the behaviour of $M_{11}(\theta_e)$ as a function of the horizontal roughness parameter and density of the medium for normal incident radiation ($\theta_i = 0$). The simulations were carried out for five values of τ ($\frac{l}{L} = [0.25,\ 0.3,\ 0.4,\ 0.5,\ 0.75]$ for the Gc model, $H = [0.25,\ 0.375,\ 0.5,\ 0.625,\ 0.9]$ for the fBm model), and three values of packing density ($\rho = [1.0,\ 0.5,\ 0.3]$) for a void size of a single dipole.

Set 2 considered the effects due to the imaginary part of the refraction index. Simulations were carried out for films with $\rho = 1.0$, $n = 1.5$, $k = [0.01i,\ 0.1i,\ 1i]$ and $H = [0.5,\ 0.625]$.

Set 3 treated the approximation of the inhomogeneous media by a homogeneous one with an average index of refraction using the Maxwell Garnett relation [7, 6]. Simulations were carried out for films with $\rho = 1.0$, $H = [0.5,\ 0.625]$, and $N = n + ik$ computed using the Maxwell Garnett relation.

Set 4 was a follow-up study for the sets 1 and 3. The behaviour of the scattered intensity was studied as a function of the size of square-shaped voids. Simulations were carried out for films with $\rho = 0.5$, $H = 0.5$, with size of the voids $n = [2,\ 4,\ 8]$ dipoles.

Set 5 was a follow-up study for the set 1. The simulations of the set 1 were carried out for $\theta_i = 15°$, and no averaging over ϕ_e was done. This was to test the consistency of the results obtained from the set 1, especially the behaviour of the specular reflectance as a function of varying ρ.

3 Results and Discussion

3.1 Results

Figures 2 and 3 sum up the primary results of the simulations. In Fig. 2 is shown the effects due to varying density, horizontal roughness parameter and different roughness model. Figure 3 illustrates the agreement of results between porous media and solid media with index of refraction computed using the relation by Maxwell Garnett, as well as the effects due to increasing void-size. The most prominent results are:

1. The Gc and the fBm models lead to rather a different distribution of the backward scattered intensity. For the fBm model, the transition from the specular reflection to diffuse is smoother than with Gc model. For both models, the specular peak smoothens when the mean scale of the roughness increases. This agrees with the theories based on wave-optics: the directional-diffuse component of the scattered radiation starts to dominate when the scale of the roughness approaches the scale of the wavelength.

2. Approximation of the inhomogeneous media using solid geometry with the relation by Maxwell Garnett agrees with the simulations. The shape of the reflectance is not sensitive to the inhomogeneities of scale $\frac{l}{\lambda} \approx 0.05$, even for a loose geometry with $\rho = 0.3$. Decreasing density is manifested as a multiplicative factor constant over θ_e, with minor differences in the shape of the reflectance distribution.

3. While the thinness of the geometry prevents us from studying the volume scattering effects in depth, basic conclusions can be made from the behaviour of the reflectance as a function of void size. From Fig. 3b. we see that the results deviate from the effective medium approximation along with the increasing void size, but the relative deviation reduces near the specular direction. Nevertheless, more simulations for off-normal incidence and significantly increased thickness are required for a serious study of the effects due to size distribution of the inhomogeneities.

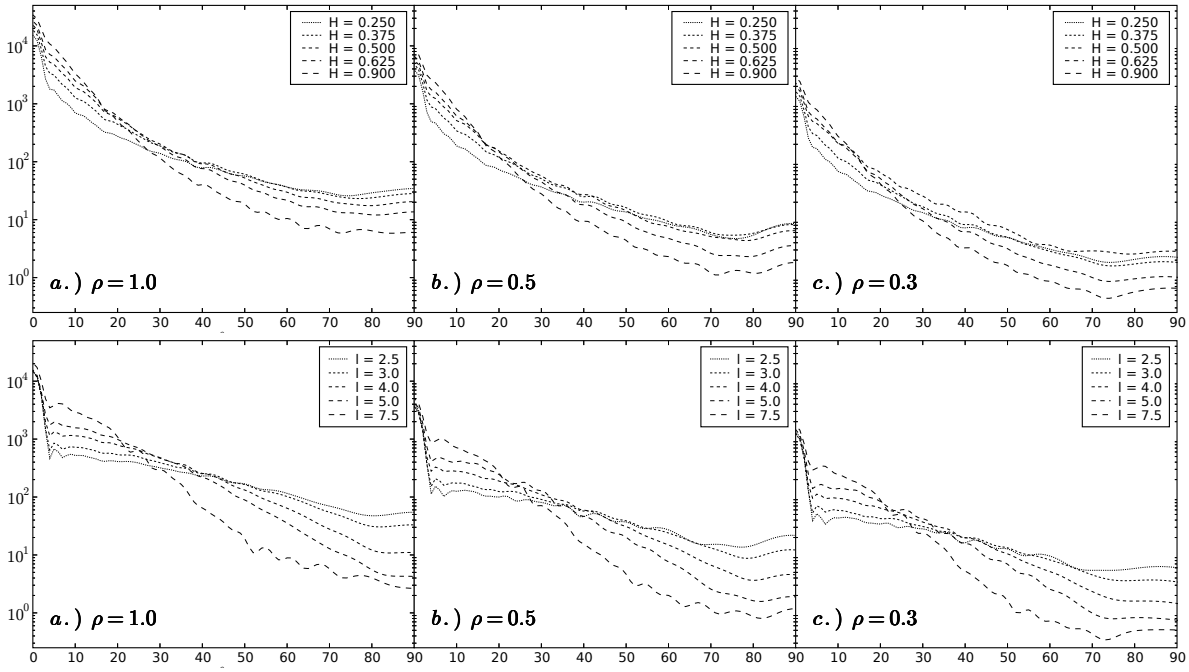

Figure 2: Distribution of the scattered intensity (M_{11}) as a function of θ_e computed for the films with fBm roughness and Gc roughness and normal incident radiation.

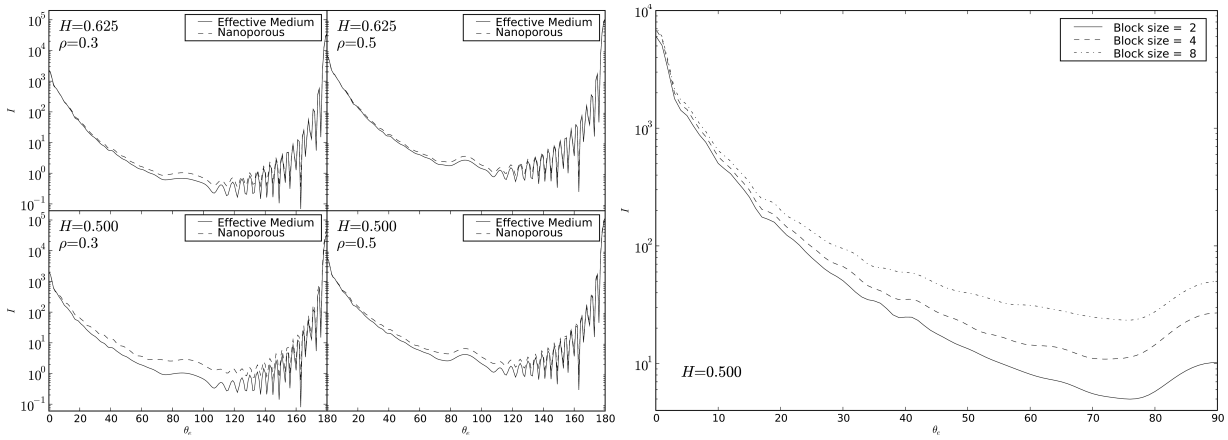

Figure 3: On the left, distribution of scattered intensity for inhomogeneous films with $\rho = [0.5,\ 0.3]$, and solid films with effective index of refraction. On the right, the effects due to the increasing void size.

3.2 Discussion

The study considered light scattering from simple nanoporous media, that is, inhomogeneous media with pore size in the nanometer range and simplified pore structure. The results can be generalized to situtations where the pore size is very small compared to other structures of the media—such as the surface roughness—and to the wavelength of the radiation. The results can not be generalized to particulate media with coherent particle structure, or to porous media with pore structure exceeding the scale of the wavelength.

Possible sources of error include the dominance of the surface dipoles over the total dipole count of the volume, and the use of normal incidence. The latter makes the separation between backscattering, directional-diffuse and the specular reflectance effects impossible

For a scattering object to be considered analogous to a surface, we must have $\frac{r}{t} >> 1$. Here r is the radius of the cylinder, and t the thickness. This is especially important for off-normal incident radiation, since the cylinder walls contribute to the scattering. Nevertheless, to include realistic volume scattering effects, we would like to have $t >> \lambda$, where λ is the wavelength of the radiation. With DDSCAT, The size of the geometry is restricted by the available memory of a single computing node. This imposes a strict limit to the geometry thickness. This limit can be raised by applying codes with capability to slice the geometry between different nodes, such as ADDA. Geometry slicing will allow us to maximize $\frac{r}{t_s}$ for a single computing node, where t_s is the thickness of a slice, and use appropriate number of nodes to achieve the total thickness.

The use of more extended rough-surface analogs will allow for the comparison between the different analytic wave-optics approximations for random rough surfaces [8] and independent numerical simulations.

References

[1] M. A. Yurkin, A. G. Hoekstra, "User Manual for the Discrete Dipole Approximation Code 'Amsterdam DDA'", 2007

[2] R. J. Adler, *The Geometry of Random Fields*, Wiley, 1981.

[3] H. P. Parviainen, *Ray tracing model for light scattering from self-affine random rough surfaces*, Master's thesis, University of Helsinki (2006).

[4] H. P. Parviainen, K. Muinonen, "Rough-surface shadowing of self-affine random rough surfaces", J. Quant. Spectros. Radiat. Transf. (2007), doi:10.1016/j.jqsrt.2007.01.025.

[5] B. T. Draine, "The discrete-dipole approximation and its application to interstellar graphite grains", ApJ **333**, 848 (1988).

[6] C. F. Bohren, D. R. Huffman, *Absorbtion and Scattering of Light by Small Particles*, Wiley, 1998

[7] J. C. Maxwell Garnett, "Colours in Metal Glasses and in Metallic Films", Phil. Trans. R. Soc. A **203**, 385 (1904)

[8] T. M. Elfouhaily, C.-A. Guérin, "TOPICAL REVIEW: A critical survey of approximate scattering wave theories from random rough surfaces", Waves in Random Media 14, 1 (2004).